

# MIMONet: Multi-Input Multi-Output On-Robot Deep Learning

Zexin Li<sup>1</sup>, Xiaoxi He<sup>2</sup>, Yufei Li<sup>1</sup>, Wei Yang<sup>3</sup>, Lothar Thiele<sup>4</sup>, and Cong Liu<sup>1</sup>

**Abstract**—Future intelligent robots are expected to process multiple inputs simultaneously (such as image and audio data) and generate multiple outputs accordingly (such as gender and emotion), similar to humans. Recent research has shown that multi-input single-output (MISO) deep neural networks (DNN) outperform traditional single-input single-output (SISO) models, representing a significant step towards this goal. In this paper, we propose MIMONet, a novel on-device multi-input multi-output (MIMO) DNN framework that achieves high accuracy and on-device efficiency in terms of critical performance metrics such as latency, energy, and memory usage. Leveraging existing SISO model compression techniques, MIMONet develops a new deep-compression method that is specifically tailored to MIMO models. This new method explores unique yet non-trivial properties of the MIMO model, resulting in boosted accuracy and on-device efficiency. Extensive experiments on three embedded platforms commonly used in robotic systems, as well as a case study using the TurtleBot3 robot, demonstrate that MIMONet achieves higher accuracy and superior on-device efficiency compared to state-of-the-art SISO and MISO models, as well as a baseline MIMO model we constructed. Our evaluation highlights the real-world applicability of MIMONet and its potential to significantly enhance the performance of intelligent robotic systems.

## I. INTRODUCTION

Single-input single-output (SISO) deep neural networks (DNNs) have demonstrated impressive performance in various robotics applications [1, 2, 3, 4]. However, multi-input single-output (MISO) DNNs have emerged as a promising alternative, as they have been shown to surpass SISO DNNs both theoretically and empirically [5, 6, 7]. Developing MISO DNNs is a crucial step towards creating multi-input multi-output (MIMO) DNNs for intelligent embedded systems, especially in the field of robotics.

According to Stanford’s “Artificial Intelligence and Life in 2030” report [8], AI is expected to impact various fields, including home services [9], healthcare [10, 11, 12, 13], and transportation [14, 15, 16, 17]. To build such robots thrive in these areas that inherently require MIMO systems, they must process real-time inputs like spoken language and facial expressions, providing personalized feedback based on factors like gender and emotion. Interactive companion robots, like the Vector Robot [18], are expected to receive camera and microphone inputs and use this information to predict user preferences and respond appropriately. In on-device learning scenarios with strict hardware constraints and performance requirements, deploying multi-input multi-output (MIMO) deep neural networks (DNNs) can be ad-

vantageous. By reducing the need to deploy multiple single-input single-output (MISO) DNN instances on the device, MIMO DNNs can significantly lower resource demands. This paper presents MIMONet, a novel on-device MIMO DNN framework that achieves both high accuracy and on-device efficiency in terms of critical performance metrics including latency, energy, and memory usage. The MIMO approach inherently offers speed improvements by requiring only one forward pass for multiple tasks (instead of multiple passes), reducing computational redundancy.

We first constructed a baseline MIMO DNN model and observed that it requires high memory consumption and struggles to meet real-time constraints due to computational demand. To minimize resource demands, MIMONet builds on an existing DNN model compression technique, VIB [19], which is effective for single-input single-output (SISO) DNN models. However, extending VIB to MIMO DNN models posed two new challenges. First, VIB exclusively supports the compression of feed-forward networks [20], which makes it unsuitable for more advanced networks, such as ResNet [21]. To address this limitation, MIMONet extends and develops a modified compression method for ResNet with residual blocks. Second, VIB was not designed to handle MIMO scenarios and did not account for the unique characteristics of MIMO models. VIB focuses on reducing intra-model redundancy but is unable to address common inter-model redundancy in MIMO models. To address this issue, MIMONet develops a new deep-compression method that reduces both inter- and intra-model redundancy, resulting in deeper lossless compression for MIMO scenarios.

We conducted a two-fold evaluation of MIMONet. First, we compared its accuracy against state-of-the-art SISO and MISO models using the RAVDESS dataset [22], showing that MIMONet outperforms them in most scenarios. In the second set, we conducted a comprehensive evaluation of MIMONet’s components’ impacts on on-device efficiency, including memory, latency, and energy. We deployed MIMONet on three widely used embedded system platforms: NVIDIA Jetson Nano Orin, NVIDIA AGX Xavier, and NVIDIA AGX Orin, which are most recent used platforms for various robotics applications [1, 2, 3, 23] such as Duckiebot [24], SparkFun Jetbot [25], and Waveshare Jetbot [26]. In addition, we evaluated MIMONet on a PC machine for a more comprehensive assessment. In summary, experimental results demonstrate that MIMONet can achieve:

- **Reduced Memory Usage:** MIMONet significantly reduces runtime memory usage by 80.7% compared to the baseline MISO models.
- **Improved Inference Speed:** MIMONet exhibits speed-

<sup>1</sup>Authors are with the University of California, Riverside.

<sup>2</sup>Authors are with the University of Macau.

<sup>3</sup>Authors are with the University of Texas at Dallas.

<sup>4</sup>Authors are with the ETH Zurich.

ups of 1.98x, 2.29x, and 1.23x compared to the baseline MISO model when tested on Nano, AGX, and Orin, respectively.

- **Enhanced Energy Efficiency:** The energy savings offered by MIMONet are 2.01x, 8.64x, and 2.71x compared to the baseline MISO model when tested on Nano, AGX, and Orin, respectively.

The major contributions of this paper can be summarized as follows:

- **Innovative MIMO Framework for Robotics:** We introduce MIMONet, one of the first frameworks to utilize a unified neural network for processing multiple inputs and outputs simultaneously, addressing complex inference tasks in robotics.
- **New Deep-Compression Method:** MIMONet implements a novel deep-compression method that enhances accuracy and on-device efficiency, specifically tailored for MIMO applications in robotics.
- **Extensive Experimental Results:** Our experiments on three embedded platforms and a PC demonstrate MIMONet’s high accuracy and superior on-device efficiency in terms of latency, energy, and memory usage, making it suitable for robots under stringent hardware constraints.
- **Real-World Case Study Validation:** We conducted a realistic case study using the TurtleBot3 robot, showing MIMONet’s practical applicability and superiority over state-of-the-art SISO and MISO models in face and audio recognition within cluttered environments. This further validates its effectiveness for interactive robotic systems.

## II. BACKGROUND AND RELATED WORK

### A. MIMO Architecture

Classical deep neural networks typically follow a single-input single-output (SISO) format, designed to process one input and produce one output at a time. However, as deep learning has evolved, certain networks have been adapted to handle multiple inputs from varied domains, enhancing accuracy. This approach, often referred to as multimodal learning [27] or multi-view learning [28], leads to what is termed multi-input single-output (MISO) networks [5, 6, 7, 29]. Building on this, models with advanced accuracies have progressed to multi-input-multi-output (MIMO) configurations [30], which are capable of generating several outputs in one go. This MIMO technology is particularly beneficial in fields like autonomous driving [31, 32] and robotic navigation [33], although it does come with substantial demands on memory and computational resources. Few concurrent works like BEVFusion [31], try to alleviate these demands by optimizing data processing from sensors to mitigate performance issues. Different from these works, our study aims to tackle these challenges by focusing on model compression to facilitate practical deployment in real-world scenarios.

### B. Model Compression for On-device Scenarios

Modern DNNs, like the ViT-Huge [34] and GPT-3 [35], although achieving state-of-the-art accuracy strain memory and computation resources for resource-constrained devices during inferences. A practical solution to mitigate such an issue is model compression, which aims to reduce model parameter count without affecting accuracy. They can involve removing redundant parameters [19, 36, 37, 38, 39] or minimizing redundant precision [40]. Two subclasses of model compression for multi-branch models consist of single-model pruning and cross-model compression. The former compresses a single network by eliminating unnecessary operations and parameters, while the latter minimizes inter-model redundancy by identifying and removing shared parameters and operations across models [19, 36, 37, 38, 41, 42, 43, 44]. Notably, the Multi-Task Zipping (MTZ) approach has pioneered cross-model compression by automating the merging of pre-trained DNNs [36]. However, MIMONet leverages the Variational Information Bottleneck (VIB) method to reduce intra-model redundancy, extending it for application to ResNet architecture. Furthermore, it adapts modified MTZ to reduce inter-model redundancy, which further decrease the total parameters in the proposed MIMO model.

## III. METHODOLOGY

### A. Overview of MIMONet

Fig. 1 illustrates an overview of the on-device MIMO inference framework. First, inspired by the famous multi-branch architecture ResNext [45], we adopt a MIMO deep neural network with multiple inputs backbone and multiple outputs classifiers as our baseline model (as shown in the first block). One forward prediction of this network requires multiple inputs (image and speech) and generates multiple prediction outputs (emotion and gender) simultaneously. To align and fuse feature information from the input image and speech, we use ResNet as the backbone to extract features from both modalities. The feature maps from both are then concatenated to create a unified representation. This fused feature map serves as the input for the subsequent prediction layers.

However, directly deploying such baseline MIMO models to embedded devices remains challenging. Specifically, embedded devices including most robots have *limited memory* and require *real-time performance* for many real-world scenarios. For instance, handling streaming data (e.g. high-speed cameras sampling 60 times per second) and ensuring robustness in safe-critical scenarios (e.g., autonomous driving robots [24, 46, 47, 48, 49]). In addition, *energy savings* are particularly needed for embedded devices because of limited battery capacity and heat dissipation.

To address these challenges, employing model compression is an intuitive and effective direction. First, we adopt the idea of VIB [19] to perform channel-wise hard masking (the masked channel generates zero output – which can be pruned, while the unmasked channel’s output remains the same) and follow pruning. Then, the pruned MIMO model

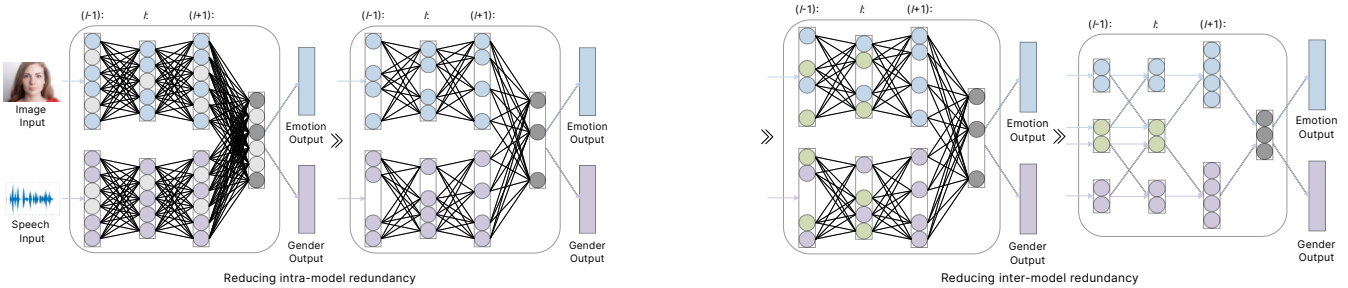


Fig. 1: Overview of MIMONet. In the left part, gray circles represent neurons inducing intra-model redundancy. In the right part, green circles denote sharable neurons inducing inter-model redundancy. Best viewed in color.

can maintain the original structure in the forward direction. However, VIB is designed for the SISO model and thus reduces the intra-model redundancy. However, it does not consider the characteristics of the MIMO framework, for instance, the MIMO framework is naturally multi-branching and exhibits inter-model redundancy. Therefore, aiming to reduce such redundancy intuitively can boost model compression performance. Furthermore, inspired by the idea from one cross-model compression work MTZ [36], we perform weights merging between multiple independent branches to improve model compression efficacy further. In summary, in MIMONet we focus on both intra-model redundancy and inter-model redundancy, and thus can theoretically further improve the compression effectiveness and achieve efficient on-device deployment.

### B. Reduce Intra-model Redundancy

We aim to reduce intra-model redundancy by performing single-model compression. Specifically, we adopt and extend the idea from VIB [19] that reduces the redundant mutual information between adjacent layers within the model. The vanilla VIB only applies to neural networks such as VGG [50]. However, when dealing with neural networks that possess a non-linear architecture, such as ResNet [21], which forms the foundation of our MIMO model, the direct application of the conventional VIB approach is not feasible.

To address this, the design incorporates an “information bottleneck” — a learnable mask — into each layer of the network that possesses learnable parameters (e.g., convolutional layers). This bottleneck selectively filters information flow between layers, allowing only the most relevant features to pass through, thus reducing redundancy. As shown in the left part of Fig. 1, neurons with gray color are masked. Furthermore, combining the characteristics of ResNet, we designed the following adaption scheme detailed in Fig. 2: (1) Module-level design: we add the information bottleneck layer as in the original VIB design for the layers not in the residual block. However, we keep the input/output channel number unchanged for each residual block, i.e., we do not insert an information bottleneck layer between two residual blocks. (2) Block-level design: After the second information bottleneck layer, we insert a *channel-recover* operation. This operation restores the channel to the pre-pruning mask based on the pruning mask by filling pruned channels with zeros, which ensures that the input channel is matched during

the concatenation operation between the main branch and the bypass. Inspired by the design idea of ResNet [21], we intuitively assume the major information throughout the network is concentrated in the bypass (consisting of direct input or input after downsampling). Therefore, we do not set the mask in the bypass section.

The surprising result of this design is that according to top-5 layer-wise compression statistics upon application to the baseline MIMO model, the image branch is (100.0%, 98.4%, 97.9%, 96.1%, 87.1%), and the speech branch is (100.0%, 100.0%, 99.4%, 92.2%, 86.7%). The information bottleneck within the residual block naturally led to all output channels except the bypass from preceding layers being masked when a high compression rate was achieved, suggesting that the primary information indeed flows through the bypass. This outcome serves as empirical validation for the assumption underlying the adapted VIB approach for ResNet. The effectiveness of this method is further supported by the observed layer-wise compression rates, indicating the potential for significant model size reduction without compromising the essential information flow through the network.

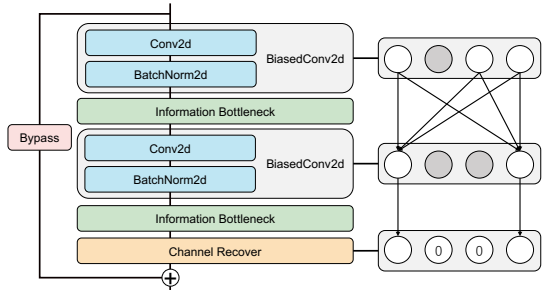


Fig. 2: Design for compression of the residual block for ResNet [21]. The left side shows the structure of the residual block. The right side shows channel-level pruning and recovery. White and gray circles exhibit kept/pruned channels. The pruned channels are filled with zeros before the feature map summing. Best viewed in color.

Furthermore, we integrate performance optimization in the residual block to collapse each convolutional (Conv2d) layer and the subsequent batch normalization (BatchNorm2d) layer into a biased convolutional (BiasedConv2d) layer, as shown in the blue box in Fig. 2. Since the on-device deployed models mainly only require forward inference, i.e., all parameters are fixed. Therefore, we could replace the

BatchNormalization (BN) layer [51] with multiplication and addition. Specifically, the output of the BN layer applied on the  $i$ -th channel of layer  $l$  is:

$$BN(y_{l,i}) = \gamma_{l,i} \cdot \frac{y_{l,i} - \mu_{l,i}}{\sqrt{\sigma_{l,i}^2 + \epsilon}} + \beta_{l,i} \quad (1)$$

where  $y_{l,i}$  is the pre-activation output of the convolution layer,  $\gamma_{l,i}$  and  $\beta_{l,i}$  are the two learnable parameters (scaling and shifting) for the BN layer,  $\mu_{l,i}$  and  $\sigma_{l,i}$  are the pre-calculated mean and standard deviation. The effect of the BN layer can be replaced by multiplying the incoming weight of convolutional layer  $w_{l,i}$  by a scalar  $\frac{\gamma_{l,i}}{\sigma_{l,i}}$  and adding  $\beta_{l,i} - \frac{\gamma_{l,i} \cdot \mu_{l,i}}{\sigma_{l,i}}$  to the bias  $b_{l,i}$ .

### C. Reduce Inter-model Redundancy

After reducing intra-model redundancy, we explore the possibility of decreasing the total number of parameters by reducing the inter-model redundancy through cross-model compression techniques. In a MIMO model, it is not obvious that sharable knowledge exists between the network’s branched parts, as they are processing inputs from an entirely different domain, e.g., one for audio and the other for video input. However, as shown in [52], sharable knowledge still exists within models designed for different input domains, as long as their outputs are fused and serve the same output tasks. Specifically, we have observed a significant amount of sharable knowledge can be found within the later layers, as features are becoming more abstract at this stage, and these abstract features are used for the same tasks.

To this end, we extend the MTZ [36, 52] framework to merge model weights from multiple independent branches. MTZ is a framework that automatically and adaptively merges deep neural networks for cross-model compression via neuron sharing. The core of MTZ is the neural similarity metric, derived from a second-order analysis of the model parameters. It measures the similarity in function between two neurons’ incoming weights, which is given by:

$$d[\tilde{\mathbf{w}}_{l,i}^A, \tilde{\mathbf{w}}_{l,j}^B] = \frac{1}{2}(\tilde{\mathbf{w}}_{l,i}^A - \tilde{\mathbf{w}}_{l,j}^B)^\top \cdot \left( (\tilde{\mathbf{H}}_{l,i}^A)^{-1} + (\tilde{\mathbf{H}}_{l,j}^B)^{-1} \right)^{-1} \cdot (\tilde{\mathbf{w}}_{l,i}^A - \tilde{\mathbf{w}}_{l,j}^B) \quad (2)$$

where  $\tilde{\mathbf{w}}_{l,i}^A, \tilde{\mathbf{w}}_{l,j}^B \in \mathbb{R}^{\tilde{N}_{l-1}}$  are the incoming weights, and  $\tilde{\mathbf{H}}_{l,i}^A, \tilde{\mathbf{H}}_{l,j}^B$  are the associated layer-wise Hessians [36, 52].

Motivated by this principle, we treat each branch as independent computing sub-graphs in our MIMO model. As shown in the right part of Fig. 1, neurons with green color are shared between different branches. The branches are aligned from the very first layer such that they can be merged and optimized by MTZ layer after layer. This design can also deal with branched layers with different widths, as long as they share the same underlying structure, such as convolutional layers or residual blocks. As proved by experiments, reducing inter-model redundancy effectively reduces the baseline MIMO model size for more efficient on-device deployment.

### D. Integrate with Quantization Techniques

To further enhance the on-device deployment efficiency of our MIMO inference framework, integrating quantization techniques presents a promising avenue. Quantization involves converting a model’s floating-point weights and activations to lower precision formats, such as fixed-point integers, which significantly reduces the model size. This process is crucial for embedded devices with stringent memory and computational resource constraints.

Our proposed method, which already incorporates strategies for intra-model and inter-model redundancy reduction, can naturally extend to include quantization. In the quantization process, the weights and activations of the pruned and merged MIMO model are mapped from floating-point to fixed-point representation. This mapping can be achieved through various quantization schemes, such as uniform or non-uniform quantization, with or without re-training (quantization-aware training or post-training quantization). For instance, post-training quantization could be directly applied to the compressed model to quickly reduce its precision without the need for further training. Specifically, for a parameter  $w$ , the quantization to 8-bit (int8) and 4-bit (int4) integers can be expressed as:

$$w_{\text{int8}} = \text{round} \left( \frac{w - \min(W)}{\max(W) - \min(W)} \times 255 \right) - 128$$

$$w_{\text{int4}} = \text{round} \left( \frac{w - \min(W)}{\max(W) - \min(W)} \times 15 \right) - 8$$

where  $W$  represents the set of all parameters in the model that are subject to quantization,  $\min(W)$  and  $\max(W)$  denote the minimum and maximum model parameters, respectively. This process introduces a trade-off between efficiency and accuracy. The integration with quantization techniques not only further reduces the memory footprint and computational requirements of the MIMO model but also leverages the hardware accelerators often found in embedded devices, which are optimized for low-precision arithmetic operations. Consequently, this integration can lead to significant improvements in inference speed and energy efficiency, making our MIMO inference framework even more suitable for real-time applications on resource-constrained devices.

## IV. EVALUATION

### A. Experimental Setup

We set up four baselines for comparison with MIMONet: two SISO models and two MISO models, both using ResNet-18 as the backbone. In MISO models, ResNet-18 extracts



Fig. 3: Data examples of RAVDESS dataset [22].

TABLE I: Experimental results of MIMONet. The best results are highlighted in bold. The second-best results are underlined.

Method	Acc./emo	Acc./gen	Par.( $\times 10^6$ )	Mem.(MB)	Latency(ms)			Energy(mJ)		
					Nano	AGX	Orin	Nano	AGX	Orin
SISO/img-emo	62.45	N/A	11.82	1003.49	6.24	7.46	2.42	49.30	298.40	134.56
SISO/img-gen	N/A	77.40	11.82	1000.12	6.04	7.50	2.38	47.60	298.02	131.76
SISO/aud-emo	61.81	N/A	11.82	983.49	3.04	4.30	1.92	24.20	171.90	71.62
SISO/aud-gen	N/A	<b>88.24</b>	11.82	956.92	2.98	4.16	1.88	23.62	166.42	70.12
MISO/emo	73.04	N/A	25.51	1362.10	10.08	8.30	3.36	80.24	348.60	161.28
MISO/gen	N/A	77.43	25.51	1342.87	9.78	8.22	3.30	77.76	343.58	158.60
MIMO	74.26	83.99	25.51	1364.96	5.26	4.15	2.95	39.98	175.29	81.90
<b>MIMONet (FP32)</b>	76.28	83.17	0.92	910.11	5.21	3.96	2.84	40.88	45.93	66.17
<b>MIMONet (FP16)</b>	76.29	83.16	0.92	688.15	5.15	3.72	2.81	40.42	43.15	61.54
<b>MIMONet (INT8)</b>	<b>76.40</b>	84.48	<u>0.92</u>	<u>577.17</u>	<u>5.11</u>	<u>3.66</u>	<u>2.74</u>	<u>39.96</u>	<u>41.34</u>	<u>59.98</u>
<b>MIMONet (INT4)</b>	75.72	<u>87.01</u>	<b>0.92</b>	<b>521.68</b>	<b>5.02</b>	<b>3.61</b>	<b>2.70</b>	<b>39.26</b>	<b>40.07</b>	<b>59.01</b>

features from each input (image and audio), which are then concatenated and passed through three fully connected layers for prediction. MIMONet differs by having multiple predictors after the fully connected layers, enabling it to generate multiple predictions in a single forward pass. We also apply approximations like half-precision (FP16) and post-training quantization (INT8 and INT4).

We leverage the RAVDESS dataset [22], with 7356 multi-modal clips from 24 actors, to evaluate our method’s performance in multi-input scenarios, specifically for concurrent emotion and gender predictions. Some examples are shown in Fig. 3. We use 80% of the data (19 actors) for training and 20% (the other 5 actors) for testing. All experiments are run three times, with averaged results reported. Such tasks are pivotal for developing robots designed for human-robot interactions, applicable in healthcare for patient monitoring by interpreting emotions, in customer service for personalized assistance, and in education to tailor teaching strategies based on emotional and demographic insights.

### B. Metrics

We study the following five metrics to evaluate the accuracy and on-device efficiency of MIMONet. 1) Accuracy: the ratio of correctly identified samples in the test set to the total number of samples in the test set. Note that the accuracies of the two tasks (emotion and gender) are evaluated separately. 2) Parameter number: number of learnable parameters. 3) Memory: required runtime memory for models. 4) Latency: average wall-clock time required to perform one forward prediction. 5) Energy: We measure system-wide energy consumption. For a fair comparison, we calculate the average latency and energy consumption for 10,000 forward passes. We aim to improve on-device efficiency (reduce parameter number, latency, memory, and energy) as much as possible while maintaining the model’s effectiveness (accuracy).

### C. Effectiveness

Table I provides a comparative analysis of the MIMONet’s performance against its SISO and MISO counterparts on the RAVDESS dataset. Observably, MIMONet and its variants with different precision (FP32, FP16, INT8, and INT4) consistently outperform SISO and MISO configurations across several metrics:

- **Accuracy:** MIMONet models demonstrate superior performance, with the INT8 variant achieving the highest emotion recognition accuracy (Acc./emo) at 76.40%, surpassing SISO and MISO models by 3.36% and a relative gain of 4.6%. The best gender recognition accuracy (Acc./gen) is 87.01%, competitive with state-of-the-art results. Although SISO models excel in gender recognition using vocal features alone, adding image inputs can introduce variability, as facial cues are not always distinct. Nevertheless, MIMONet maintains excellent recognition ability even after compression due to ResNet’s efficient feature extraction and fusion of image and audio inputs. Compression techniques like INT8 further enhance efficiency by reducing resource requirements while preserving high accuracy, showcasing MIMONet’s adaptability in processing multi-modal data.
- **Parameter number (Par.):** MIMONet largely reduce parameter number via reducing intra- and inter-task redundancies. It can reach a 96.4% compression rate while achieving very competitive accuracy performance.
- **Memory Usage (Mem.):** MIMONet demonstrates significant memory efficiency for memory-constrained robotic scenarios. For instance, while MISO/emo and MISO/gen configurations require about 1362.10 and 1342.87 MB of memory respectively, the MIMONet variants operate with markedly less, with the MIMO (INT4) requiring only 521.68 MB. Note that MIMO can operate both tasks simultaneously, unlike the two separate MISO models, which in total consume 2704.97 MB<sup>1</sup>, representing approximately up to **80.7%** reductions<sup>2</sup> in memory requirements compared to MISO models.
- **Latency (Latency/FP):** MIMONet shows better latency performance on all three embedded testbeds. Note that MIMONet could generate results of two tasks in one forward pass, while SISO or MISO requires two forward

<sup>1</sup>The 2704.97 MB memory usage for two MISO models may double-count shared PyTorch framework memory. In practice, models can share some memory, reducing the total. However, MIMONet still provides substantial memory savings.

<sup>2</sup>Although the parameter count of MIMONet is reduced by up to 96.4%, memory consumption is not reduced by as much. This is because the PyTorch framework reserves some internal memory and introduces memory overhead.

TABLE II: Ablation study results of accuracy and on-device efficiency. The best results are in bold.

Method	Acc./emo	Acc./gen	Par.( $\times 10^6$ )	Mem.(MB)	Latency(ms)			Energy(mJ)		
					Nano	AGX	Orin	Nano	AGX	Orin
<b>MIMONet</b>	<b>76.40</b>	<b>84.48</b>	<b>0.92</b>	<b>577.17</b>	<b>5.11</b>	<b>3.66</b>	<b>2.74</b>	<b>39.96</b>	<b>41.34</b>	<b>59.98</b>
w/o VIB	74.26	83.99	25.51	1364.96	5.26	4.15	2.95	39.98	175.29	81.90
w/o MTZ	75.63	82.70	1.07	930.09	5.15	3.98	2.80	40.28	44.23	62.34
w/o PTQ	76.28	83.17	0.92	910.11	5.32	3.96	2.84	40.88	45.93	66.17
<b>MIMONet</b>	<b>76.40</b>	<b>84.48</b>	<b>0.92</b>	<b>577.17</b>	<b>5.11</b>	<b>3.66</b>	<b>2.74</b>	<b>39.96</b>	<b>41.34</b>	<b>59.98</b>
w/ RandPruning	12.66	51.22	0.92	579.22	5.15	3.71	2.77	40.43	42.23	60.12

passes. Specifically, MIMONet exhibits speedup compared to MISO models up to 1.98x, 2.29x, and 1.23x on Nano, AGX, and Orin, respectively.

- **Energy (Energy/FP):** MIMONet also demonstrates superior efficiency on all three embedded testbeds. Specifically, MIMONet exhibits energy saving compared to MISO models up to 2.01x, 8.64x, and 2.71x on Nano, AGX, and Orin, respectively.

*Effective and Efficient on-device deployment:* our experimental results demonstrate that MIMONet can address all challenges in Sec. III-A (limited memory, real-time constraints, and energy constraints) while not sacrificing and often improving accuracy performance.

#### D. Ablation Study

We exhibit the ablation study results in Table II. We interpret the results as follows:

- **Efficacy of Reducing Intra-Task Redundancy (VIB):** Removing VIB increases memory usage from 577.17 MB to 1364.96 MB and parameters from 0.92 million to 25.51 million, highlighting its effectiveness in reducing intra-task redundancy. Unlike random pruning, which largely degrades accuracy, VIB retains relevant information and reduces noise, making it crucial and particularly work for managing MIMO tasks efficiently.
- **Efficacy of Reducing Inter-Task Redundancy (MTZ):** Omitting MTZ reduces accuracy in emotion and gender recognition, increases memory usage, and raises latency slightly, demonstrating its importance in minimizing inter-task redundancy and maintaining accuracy.
- **Efficacy of Post-Training Quantization (PTQ):** PTQ significantly reduces the model footprint through low-precision data structures, with minimal impact on accuracy. It decreases latency and energy consumption, enhancing post-training efficiency without major accuracy loss.

*Component Efficacy:* The ablation study confirms the critical role of each MIMONet component in ensuring optimal on-device performance.

#### E. Case study on TurtleBot3

We conduct a case study using the TurtleBot3 robot to evaluate the real-world applicability of MIMONet. Specifically, we replace the TurtleBot3’s main control device with a Jetson Nano and install an RGB camera, USB audio card, and speakers. Subsequently, a native speaker was invited

to converse with the robot using happy tones while facial videos were captured. The robot will make sounds and specific movements based on the predictions. We evaluate three models (MISO, vanilla MIMO, and MIMONet) and find that MISO generated wrong results and exhibited the longest response time due to two-pass inferences. In contrast, vanilla MIMO and MIMONet both yield accurate results, while MIMONet yields significantly shorter response times (3.00x speedup than vanilla MIMO on average), which aligns with our evaluation (Sec. IV-C and Sec. IV-D).

#### V. DISCUSSION ON FUTURE DIRECTIONS

Recent research on model compression has primarily focused on simpler models, often neglecting complex architectures like ResNet [21], Transformer [53], and complex graph-based models [54, 55, 56, 57, 58, 59, 60, 61]. Neural architecture search offers promising methods for creating efficient designs suitable for rapid inference [62]. Our goal is to adapt MIMONet for these advanced architectures, optimizing them for on-device use by addressing latency, energy, and memory limitations in models [5, 6, 63, 64]. While our approach improves performance on GPU-based devices, integrating FPGAs [65, 66], autonomous vehicles [67], and emerging VR technologies [68] into AI-optimized embedded systems highlights a shift towards software-hardware co-design [69] for heterogeneous computing, paving the way for broader on-device model deployment. In complex and diverse multi-task models, compression gains might diminish with less overlap between complex multiple tasks. We leave this to future work, where we plan to explore adaptive compression strategies tailored for complex multi-task scenarios.

#### VI. CONCLUSION

This paper introduces MIMONet, one of the first on-device Multi-Input Multi-Output (MIMO) Deep Neural Network (DNN) frameworks targeting robotic applications. MIMONet achieves high accuracy and on-device efficiency in terms of critical performance metrics, such as latency, energy, and memory usage. Extensive experiments on three widely used embedded platforms demonstrate that MIMONet can provide high accuracy while enabling superior on-device efficiency, particularly when compared to state-of-the-art Single-Input Single-Output (SISO) and Multiple-Input Single-Output (MISO) models. Our research is an important first step toward building efficient MIMO DNN frameworks for practical on-device learning scenarios, particularly for robots that often face hardware and performance constraints.



## REFERENCES

- [1] X. Deng, Y. Xiang, A. Mousavian, C. Eppner, T. Bretl, and D. Fox, "Self-supervised 6d object pose estimation for robot manipulation," in *2020 IEEE International Conference on Robotics and Automation (ICRA)*. IEEE, 2020, pp. 3665–3671.
- [2] X. Meng, N. Ratliff, Y. Xiang, and D. Fox, "Neural autonomous navigation with riemannian motion policy," in *2019 International Conference on Robotics and Automation (ICRA)*. IEEE, 2019, pp. 8860–8866.
- [3] Z. Yang, A. B. Clark, D. Chappell, and N. Rojas, "Instinctive real-time semg-based control of prosthetic hand with reduced data acquisition and embedded deep learning training," in *2022 International Conference on Robotics and Automation (ICRA)*. IEEE, 2022, pp. 5666–5672.
- [4] S. Su, Y. Li, S. He, S. Han, C. Feng, C. Ding, and F. Miao, "Uncertainty quantification of collaborative detection for self-driving," *arXiv preprint arXiv:2209.08162*, 2022.
- [5] W. Wang, H. Bao, L. Dong, J. Bjorck, Z. Peng, Q. Liu, K. Aggarwal, O. K. Mohammed, S. Singhal, S. Som, and F. Wei, "Image as a foreign language: Beit pretraining for all vision and vision-language tasks," *CoRR*, vol. abs/2208.10442, 2022.
- [6] S. E. Reed, K. Zolna, E. Parisotto, S. G. Colmenarejo, A. Novikov, G. Barth-Maron, M. Gimenez, Y. Sulsky, J. Kay, J. T. Springenberg, T. Eccles, J. Bruce, A. Razavi, A. Edwards, N. Heess, Y. Chen, R. Hadsell, O. Vinyals, M. Bordbar, and N. de Freitas, "A generalist agent," *CoRR*, vol. abs/2205.06175, 2022.
- [7] R. Hu and A. Singh, "Unit: Multimodal multitask learning with a unified transformer," in *2021 IEEE/CVF International Conference on Computer Vision, ICCV 2021, Montreal, QC, Canada, October 10-17, 2021*. IEEE, 2021, pp. 1419–1429.
- [8] P. Stone, R. Brooks, E. Brynjolfsson, R. Calo, O. Etzioni, G. Hager, J. Hirschberg, S. Kalyan Krishnan, E. Kamar, S. Kraus, et al., "Artificial intelligence and life in 2030: the one hundred year study on artificial intelligence," *arXiv preprint arXiv:2211.06318*, 2022.
- [9] B.-J. You, M. Hwangbo, S.-O. Lee, S.-R. Oh, Y. Do Kwon, and S. Lim, "Development of a home service robot'issac,'" in *Proceedings 2003 IEEE/RSJ International Conference on Intelligent Robots and Systems (IROS 2003)(Cat. No. 03CH37453)*, vol. 3. IEEE, 2003, pp. 2630–2635.
- [10] H. Ma, D. Zeng, and Y. Liu, "Learning optimal group-structured individualized treatment rules with many treatments," *Journal of Machine Learning Research*, vol. 24, no. 102, pp. 1–48, 2023.
- [11] —, "Learning individualized treatment rules with many treatments: A supervised clustering approach using adaptive fusion," *Advances in Neural Information Processing Systems*, vol. 35, pp. 15956–15969, 2022.
- [12] W. Lyu, X. Dong, R. Wong, S. Zheng, K. Abell-Hart, F. Wang, and C. Chen, "A multimodal transformer: Fusing clinical notes with structured ehr data for interpretable in-hospital mortality prediction," in *AMIA Annual Symposium Proceedings*, vol. 2022. American Medical Informatics Association, 2022, p. 719.
- [13] W. Lyu, Z. Bi, F. Wang, and C. Chen, "Badclm: Backdoor attack in clinical language models for electronic health records," *arXiv preprint arXiv:2407.05213*, 2024.
- [14] X. Ma, A. Karimpour, and Y.-J. Wu, "Eliminating the impacts of traffic volume variation on before and after studies: a causal inference approach," *Journal of Intelligent Transportation Systems*, pp. 1–15, 2023.
- [15] —, "Data-driven transfer learning framework for estimating on-ramp and off-ramp traffic flows," *Journal of Intelligent Transportation Systems*, pp. 1–14, 2024.
- [16] A. Cottam, X. Li, X. Ma, and Y.-J. Wu, "Large-scale freeway traffic flow estimation using crowdsourced data: A case study in arizona," *Journal of Transportation Engineering, Part A: Systems*, vol. 150, no. 7, p. 04024030, 2024.
- [17] Z. Zhang, Y. Sun, Z. Wang, Y. Nie, X. Ma, P. Sun, and R. Li, "Large language models for mobility in transportation systems: A survey on forecasting tasks," *arXiv preprint arXiv:2405.02357*, 2024.
- [18] Digitaldreamlabs, "Vector 2.0 ai robot companion," <https://www.digitaldreamlabs.com/products/vector-robot>, 2022.
- [19] B. Dai, C. Zhu, B. Guo, and D. Wipf, "Compressing neural networks using the variational information bottleneck," in *International Conference on Machine Learning*. PMLR, 2018, pp. 1135–1144.
- [20] G. Bebis and M. Georgiopoulos, "Feed-forward neural networks," *IEEE Potentials*, vol. 13, no. 4, pp. 27–31, 1994.
- [21] K. He, X. Zhang, S. Ren, and J. Sun, "Deep residual learning for image recognition," in *Proceedings of the IEEE conference on computer vision and pattern recognition*, 2016, pp. 770–778.
- [22] S. R. Livingstone and F. A. Russo, "The ryerson audio-visual database of emotional speech and song (ravdess): A dynamic, multimodal set of facial and vocal expressions in north american english," *PLoS one*, vol. 13, no. 5, p. e0196391, 2018.
- [23] J. Guo, A. Li, and C. Liu, "Backdoor detection and mitigation in competitive reinforcement learning," 2023.
- [24] NVIDIA, "Duckiebot (db-j)," <https://get.duckietown.com/products/duckiebot-db21>, 2022.
- [25] —, "Sparkfun jetbot ai kit," <https://www.sparkfun.com/products/18486>, 2022.
- [26] —, "Waveshare jetbot ai kit," <https://www.amazon.com/Waveshare-JetBot-AI-Kit-Accessories/dp/B07V8JL4TF/>, 2022.
- [27] S. Zhang, S. Zhang, T. Huang, and W. Gao, "Multimodal deep convolutional neural network for audio-visual emotion recognition," in *Proceedings of the 2016 ACM on International Conference on Multimedia Retrieval*, 2016, pp. 281–284.
- [28] J. Zhao, X. Xie, X. Xu, and S. Sun, "Multi-view learning overview: Recent progress and new challenges," *Information Fusion*, vol. 38, pp. 43–54, 2017.
- [29] X. He, "Towards on-device intelligence," Ph.D. dissertation, ETH Zurich, 2022.
- [30] M. Havasi, R. Jenatton, S. Fort, J. Z. Liu, J. Snoek, B. Lakshminarayanan, A. M. Dai, and D. Tran, "Training independent subnetworks for robust prediction," *arXiv preprint arXiv:2010.06610*, 2020.
- [31] Z. Liu, H. Tang, A. Amini, X. Yang, H. Mao, D. Rus, and S. Han, "Bevfusion: Multi-task multi-sensor fusion with unified bird's-eye view representation," *arXiv preprint arXiv:2205.13542*, 2022.
- [32] Z. Huang, S. Lin, G. Liu, M. Luo, C. Ye, H. Xu, X. Chang, and X. Liang, "Fuller: Unified multi-modality multi-task 3d perception via multi-level gradient calibration," in *Proceedings of the IEEE/CVF International Conference on Computer Vision*, 2023, pp. 3502–3511.
- [33] D. S. Chaplot, L. Lee, R. Salakhutdinov, D. Parikh, and D. Batra, "Embodied multimodal multitask learning," *arXiv preprint arXiv:1902.01385*, 2019.
- [34] B. Wu, C. Xu, X. Dai, A. Wan, P. Zhang, Z. Yan, M. Tomizuka, J. Gonzalez, K. Keutzer, and P. Vajda, "Visual transformers: Token-based image representation and processing for computer vision," 2020.
- [35] T. Brown, B. Mann, N. Ryder, M. Subbiah, J. D. Kaplan, P. Dhariwal, A. Neelakantan, P. Shyam, G. Sastry, A. Askell, et al., "Language models are few-shot learners," *Advances in neural information processing systems*, vol. 33, pp. 1877–1901, 2020.
- [36] X. He, Z. Zhou, and L. Thiele, "Multi-task zipping via layer-wise neuron sharing," in *Advances in Neural Information Processing Systems*, 2018, pp. 6019–6029.
- [37] X. Dong, S. Chen, and S. Pan, "Learning to prune deep neural networks via layer-wise optimal brain surgeon," in *Advances in Neural Information Processing Systems*, 2017, pp. 4860–4874.
- [38] B. Hassibi and D. G. Stork, "Second order derivatives for network pruning: Optimal brain surgeon," in *Advances in Neural Information Processing Systems*, 1993, pp. 164–171.
- [39] S. Liu, J. Du, K. Nan, Z. Zhou, H. Liu, Z. Wang, and Y. Lin, "Adadeep: A usage-driven, automated deep model compression framework for enabling ubiquitous intelligent mobiles," *IEEE Transactions on Mobile Computing*, pp. 1–1, 2020.
- [40] M. Courbariaux, Y. Bengio, and J.-P. David, "Binaryconnect: Training deep neural networks with binary weights during propagations," in *Advances in Neural Information Processing Systems*, 2015, pp. 3123–3131.
- [41] P. Molchanov, A. Mallya, S. Tyree, I. Frosio, and J. Kautz, "Importance estimation for neural network pruning," in *Proceedings of IEEE/CVF Conference on Computer Vision and Pattern Recognition*, 2019, pp. 11264–11272.
- [42] L. Deng, G. Li, S. Han, L. Shi, and Y. Xie, "Model compression and hardware acceleration for neural networks: a comprehensive survey," *Proceedings of the IEEE*, vol. 108, no. 4, pp. 485–532, 2020.
- [43] X. He, D. Gao, Z. Zhou, Y. Tong, and L. Thiele, "Pruning-aware merging for efficient multitask inference," in *Proceedings of ACM SIGKDD Conference on Knowledge Discovery & Data Mining*. New York, NY, USA: ACM, 2021, pp. 585–595.
- [44] Y.-M. Chou, Y.-M. Chan, J.-H. Lee, C.-Y. Chiu, and C.-S. Chen, "Unifying and merging well-trained deep neural networks for inference

- stage,” in *Proceedings of International Joint Conference on Artificial Intelligence*, 2018, pp. 2049–2056.
- [45] S. Xie, R. Girshick, P. Dollár, Z. Tu, and K. He, “Aggregated residual transformations for deep neural networks,” in *Proceedings of the IEEE conference on computer vision and pattern recognition*, 2017, pp. 1492–1500.
- [46] H. Zhou, W. Li, Z. Kong, J. Guo, Y. Zhang, B. Yu, L. Zhang, and C. Liu, “Deepbillboard: Systematic physical-world testing of autonomous driving systems,” in *Proceedings of the ACM/IEEE 42nd International Conference on Software Engineering*.
- [47] Z. Kong, J. Guo, A. Li, and C. Liu, “Physgan: Generating physical-world-resilient adversarial examples for autonomous driving,” 2019.
- [48] H. Song, C. Liu, and H. Dai, “Bundledslam: An accurate visual slam system using multiple cameras,” in *2024 IEEE 7th Advanced Information Technology, Electronic and Automation Control Conference (IAEAC)*, vol. 7. IEEE, 2024, pp. 106–111.
- [49] H. Song, Z. Qu, Z. Zhang, Z. Ye, and C. Liu, “Eta-init: Enhancing the translation accuracy for stereo visual-inertial slam initialization,” *arXiv preprint arXiv:2405.15082*, 2024.
- [50] K. Simonyan and A. Zisserman, “Very deep convolutional networks for large-scale image recognition,” *arXiv preprint arXiv:1409.1556*, 2014.
- [51] S. Ioffe and C. Szegedy, “Batch normalization: Accelerating deep network training by reducing internal covariate shift,” in *International conference on machine learning*. pmlr, 2015, pp. 448–456.
- [52] X. He, X. Wang, Z. Zhou, J. Wu, Z. Yang, and L. Thiele, “On-device deep multi-task inference via multi-task zipping,” *IEEE Transactions on Mobile Computing*, 2021.
- [53] A. Vaswani, N. Shazeer, N. Parmar, J. Uszkoreit, L. Jones, A. N. Gomez, L. Kaiser, and I. Polosukhin, “Attention is all you need,” in *Advances in Neural Information Processing Systems 30: Annual Conference on Neural Information Processing Systems 2017, December 4-9, 2017, Long Beach, CA, USA*, I. Guyon, U. von Luxburg, S. Bengio, H. M. Wallach, R. Fergus, S. V. N. Vishwanathan, and R. Garnett, Eds., 2017, pp. 5998–6008.
- [54] T. N. Kipf and M. Welling, “Semi-supervised classification with graph convolutional networks,” in *5th International Conference on Learning Representations, ICLR 2017, Toulon, France, April 24-26, 2017, Conference Track Proceedings*. OpenReview.net, 2017. [Online]. Available: <https://openreview.net/forum?id=SJU4ayYgl>
- [55] W. L. Hamilton, Z. Ying, and J. Leskovec, “Inductive representation learning on large graphs,” in *Advances in Neural Information Processing Systems 30: Annual Conference on Neural Information Processing Systems 2017, December 4-9, 2017, Long Beach, CA, USA*, I. Guyon, U. von Luxburg, S. Bengio, H. M. Wallach, R. Fergus, S. V. N. Vishwanathan, and R. Garnett, Eds., 2017, pp. 1024–1034.
- [56] P. Velickovic, G. Cucurull, A. Casanova, A. Romero, P. Liò, and Y. Bengio, “Graph attention networks,” in *6th International Conference on Learning Representations, ICLR 2018, Vancouver, BC, Canada, April 30 - May 3, 2018, Conference Track Proceedings*. OpenReview.net, 2018.
- [57] M. Afarin, C. Gao, S. Rahman, N. Abu-Ghazaleh, and R. Gupta, “Commongraph: Graph analytics on evolving data,” in *Proceedings of the 28th ACM International Conference on Architectural Support for Programming Languages and Operating Systems, Volume 2*, 2023.
- [58] C. Gao, M. Afarin, S. Rahman, N. Abu-Ghazaleh, and R. Gupta, “Mega evolving graph accelerator,” in *Proceedings of the 56th Annual IEEE/ACM International Symposium on Microarchitecture*, 2023.
- [59] G. Dong, “Deep graph learning in mobile health,” Ph.D. dissertation, University of Virginia, 2022.
- [60] G. Dong, Y. Kweon, B. B. Park, and M. Boukhechba, “Utility-based route choice behavior modeling using deep sequential models,” *Journal of big data analytics in transportation*, vol. 4, no. 2, pp. 119–133, 2022.
- [61] G. Dong, M. Tang, Z. Wang, J. Gao, S. Guo, L. Cai, R. Gutierrez, B. Campbell, L. E. Barnes, and M. Boukhechba, “Graph neural networks in iot: A survey,” *ACM Transactions on Sensor Networks*, vol. 19, no. 2, pp. 1–50, 2023.
- [62] Y. Zhang, D. Pandey, D. Wu, T. Kundu, R. Li, and T. Shu, “Accuracy-constrained efficiency optimization and gpu profiling of cnn inference for detecting drainage crossing locations,” in *Proceedings of the SC’23 Workshops of The International Conference on High Performance Computing, Network, Storage, and Analysis*, 2023, pp. 1780–1788.
- [63] C. Gao and S. Q. Zhang, “Dlora: Distributed parameter-efficient fine-tuning solution for large language model,” *arXiv preprint arXiv:2404.05182*, 2024.
- [64] Z. Han, C. Gao, J. Liu, S. Q. Zhang, *et al.*, “Parameter-efficient fine-tuning for large models: A comprehensive survey,” *arXiv preprint arXiv:2403.14608*, 2024.
- [65] A. Canis, J. Choi, M. Aldham, V. Zhang, A. Kammoona, J. H. Anderson, S. Brown, and T. Czajkowski, “Legup: high-level synthesis for fpga-based processor/accelerator systems,” in *Proceedings of the 19th ACM/SIGDA international symposium on Field programmable gate arrays*, 2011, pp. 33–36.
- [66] Y. Zhang, R. Yasaei, H. Chen, Z. Li, and M. A. Al Faruque, “Stealing neural network structure through remote fpga side-channel analysis,” *IEEE Transactions on Information Forensics and Security*, vol. 16, pp. 4377–4388, 2021.
- [67] G. Dong, M. Tang, R. Yan, Z. Mu, L. Cai, and B. B. Park, “Deep learning for autonomous vehicles and systems,” in *Autonomous Vehicles and Systems*. River Publishers, 2023, pp. 9–47.
- [68] C. Slocum, Y. Zhang, N. Abu-Ghazaleh, and J. Chen, “Going through the motions: {AR/VR} keylogging from user head motions,” in *32nd USENIX Security Symposium (USENIX Security 23)*, 2023.
- [69] J. Zhang, H. Gu, G. L. Zhang, B. Li, and U. Schlichtmann, “Hardware-software codesign of weight reshaping and systolic array multiplexing for efficient cnns,” in *2021 Design, Automation & Test in Europe Conference & Exhibition (DATE)*. IEEE, 2021, pp. 667–672.